

See discussions, stats, and author profiles for this publication at: <https://www.researchgate.net/publication/221883372>

Dye-Loaded Porous Nanocapsules Immobilized in a Permeable Polyvinyl Alcohol Matrix: A Versatile Optical Sensor Platform

ARTICLE *in* ANALYTICAL CHEMISTRY · FEBRUARY 2012

Impact Factor: 5.64 · DOI: 10.1021/ac2027657 · Source: PubMed

CITATIONS

18

READS

79

4 AUTHORS, INCLUDING:



Sergey A. Dergunov
University of Connecticut
32 PUBLICATIONS 331 CITATIONS

[SEE PROFILE](#)

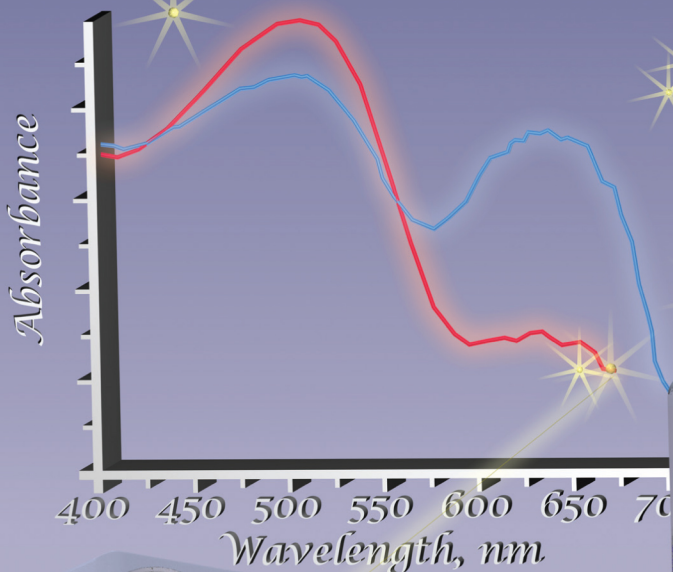


E. Lindner
The University of Memphis
146 PUBLICATIONS 4,237 CITATIONS

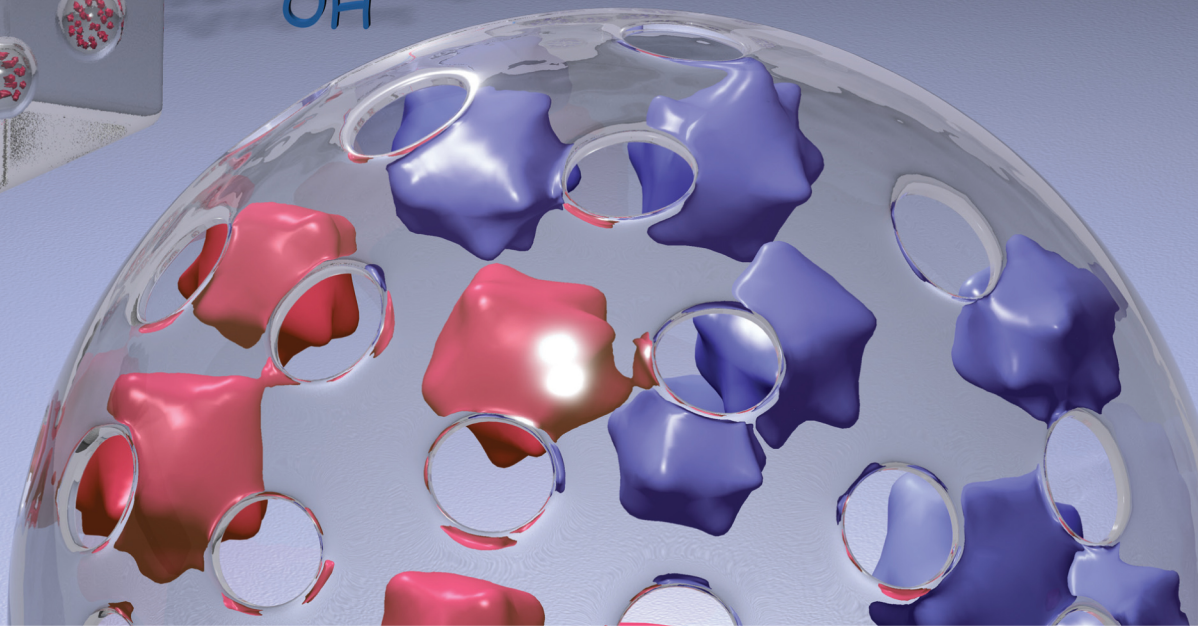
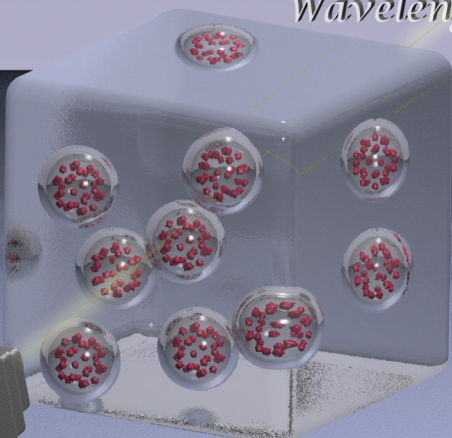
[SEE PROFILE](#)

analytical chemistry

March 20, 2012 Volume 84 Number 6



Optical Sensing with Immobilized Dye-Loaded Porous Nanocapsules



ACS Publications

MOST TRUSTED. MOST CITED. MOST READ.

www.acs.org

Dye-Loaded Porous Nanocapsules Immobilized in a Permeable Polyvinyl Alcohol Matrix: A Versatile Optical Sensor Platform

Mariya D. Kim,^{†,‡,§} Sergey A. Dergunov,^{†,‡,§} Ernö Lindner,^{*,†,||} and Eugene Pinkhassik^{*,†,‡,§}

[†]Sensor Institute of the University Memphis (SENSORIUM), Memphis, Tennessee 38152, United States

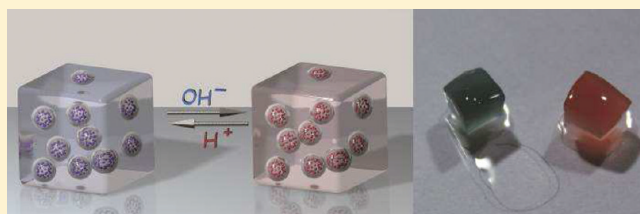
[‡]Department of Chemistry, The University of Memphis, Memphis, Tennessee 38152, United States

[§]Department of Chemistry, Saint Louis University, 3501 Laclede Avenue, St. Louis, Missouri 63103, United States

^{||}Department of Biomedical Engineering, The University of Memphis, Memphis, Tennessee 38152, United States

Supporting Information

ABSTRACT: In this work we report on a versatile sensor platform based on encapsulated indicator dyes. Dyes are entrapped in hollow nanocapsules with nanometer-thin walls of controlled porosity. The porous nanocapsules retain molecules larger than the pore size but provide ultrafast access to their interior for molecules and ions smaller than the pore size. Dye-loaded nanocapsules are immobilized in a polyvinyl alcohol (PVA) matrix with high solvent permeability and rapid analyte diffusion. This approach provides robust sensing films with fast response and extended lifetime. To demonstrate the performance characteristics of such films, pH-sensitive indicator dyes were entrapped in vesicle-templated nanocapsules prepared by copolymerization of *tert*-butyl methacrylate, butyl methacrylate, and ethylene glycol dimethacrylate. As pH sensitive dyes, Nile blue A, bromophenol blue, and acid fuchsin were tested. Time-resolved absorbance measurements showed that the rate of the color change is controlled by the rate of diffusion of protons in the hydrogel. The pH-induced color change in a ~400 μm thick film is complete within 40 and 60 s. The porous nanocapsule loaded films showed excellent stability and reproducibility in long-term monitoring experiments. Compartmentalization of the indicator dyes within the nanocapsules increased their stability. The matrix caused a shift in the position of the color change of the dye compared to that in an aqueous buffer solution. The encapsulation/immobilization protocol described in this account is expected to be broadly applicable to a variety of indicator dyes in optical sensor applications.



Chemical sensors are commonly classified as surface or bulk sensors to emphasize the importance of the signal generation process and stress the relevance of the analytical information provided by the different sensors.^{1,2} Optical sensors are generally considered as bulk sensors because the information provided by the most widely used optical transduction techniques (absorption and luminescence) is from the bulk of a solution (direct sensing) or the bulk of a sensing matrix/membrane (reagent mediated sensing). In reagent mediated sensing, the reagent is commonly embedded in a matrix or immobilized directly onto the surface of the sensing platform, e.g., on the end of an optical fiber or onto the surface of a waveguide. In the latter case, when the dye molecules (reagent or color indicator) are confined to the surface, one may argue for considering these optical sensors also as surface sensors.³

Optical sensors, in which the reagent is embedded into an inert matrix, are often characterized with sluggish response since the equilibration between the sample and the sensing matrix/membrane is mass transfer controlled.⁴ The main parameters that control the time responses of such reagent mediated optical sensors are the membrane thickness and the diffusion coefficient of the analyte in the membrane. The rate of the equilibration processes can be facilitated by decreasing the

membrane thickness of the sensing matrix and/or by selecting a sensing matrix, in which the analyte molecules have large diffusion coefficients. However, both of these approaches can have dire consequences. Optical sensors with thin membranes may not have adequate sensitivity, since the sensitivity is directly proportional to the path length. On the other hand, optical sensors in which the reagent is embedded in low-density, highly porous membranes commonly have large drift and short lifetime due to the leaching of the reagent. To minimize leaching from a sensing matrix/membrane, reagents can be immobilized to the matrix through covalent coupling. Covalent attachment offers high stability but requires the development of molecule-specific chemistries and commonly influences the properties of the immobilized dye molecule, e.g., its dissociation constant.⁴ An attractive recent approach of covalent coupling is through the utilization of nanoparticles and doping the matrix with the reagent-decorated nanoparticles.^{5,6} The hydrophobicity, pore size, and charge of the matrix determine its loading capacity and permeability, which control

Received: October 19, 2011

Accepted: February 15, 2012

Published: February 15, 2012



the sensitivity and response time of the sensing probes.⁷ The selection of the polymeric matrix^{8,9} is also important for adequate mechanical properties. The compatibility of sol–gels with optical fibers made them especially attractive for immobilization in sensor applications. However, tuning the sol–gel microstructure (primarily hydrophobicity and pore size) for short response and extended lifetime is a complex task.^{8,10} Polymer hydrogels are attractive as matrixes since they are inexpensive and easy to make and their properties can be tuned in a broad range. However, the difficulties in retaining the indicator dyes in high-porosity hydrogels limit their applications.

The possibilities for optical sensing strategies have exploded through novel optical materials and optoelectronic devices. However, certain basic limitations of optical sensors related to their spatial and time resolution and long-term stability remained.⁸ In particular, combining short response times with long-term stability in a versatile platform without the need for covalent immobilization of the low molecular weight indicator dyes remained an unsolved challenge. In this contribution, we report a novel optical sensing platform that utilizes dye-loaded, porous nanocapsules embedded in a low-density poly(vinylalcohol) matrix for pH sensing. The wall of the porous nanocapsule is so thin (approximately 1 nm) and the number of pores in the capsule wall is so large that the flux of hydronium ions in and out of the capsules is not slowed down. Consequently, free and encapsulated dye molecules change their colors at the same rate upon pH changes in the solution.¹¹ When low-density hydrogels are doped with dye-loaded nanocapsules, the rate of the color change of the gel is only controlled by the gel thickness and the diffusion coefficients of protons in the gel. The diffusion coefficient of the ~100 nm diameter nanocapsules in the gel is negligible compared to free dye molecules, i.e., no leaching from the gel could be detected. In addition, the encapsulation of the dye into the nanocapsules significantly improved the stability of the dye against photo-bleaching.

EXPERIMENTAL SECTION

Chemicals. 1,2-Dimyristoyl-sn-glycero-3-phosphocholine (DMPC) was purchased from Avanti Polar Lipids, Inc. as a dry powder. *tert*-Butyl methacrylate (*t*-BMA) and butyl methacrylate (BMA), used as monomers, and ethylene glycol dimethacrylate (EGDMA), used as a cross-linking agent, were purchased from Sigma-Aldrich and were passed through an alumina column to remove the inhibitor shortly before the polymerization. The photoinitiator 2,2-dimethoxy-2-phenyl-acetophenone (DPA), manufactured by Sigma-Aldrich, was used without any additional purification. The pH indicator dye Nile blue A (NB A), also from Sigma-Aldrich, was dissolved in tris buffer (10 mM, pH 7.4) and filtered before use. Bromophenol blue, acid fuchsin, and polyvinyl alcohol (PVA) with molecular weight 67 000 (Mowiol 8-88) were all purchased from Sigma-Aldrich and used as received. Glutaric aldehyde solution (GDA) (Sigma-Aldrich, grade II, 25% in water) was used for cross-linking PVA to form a gel matrix. The solvents and other chemicals used in this study were HPLC and ACS reagent grade, respectively, and were used as received.

Preparation of Dye-Loaded Nanocapsules. DMPC (160 mg, 0.235 mmol) was dissolved in 0.4 mL of chloroform in a test tube, then *t*-BMA (32 μ L, 0.193 mmol), BMA (32 μ L, 0.199 mmol), EGDMA (32 μ L, 0.166 mmol), and initiator 2,2-dimethoxy-2-phenyl-acetophenone (3 mg, 0.01 mmol) were

added. Chloroform was evaporated using a stream of purified argon to form a lipid/monomer mixture. Methylene chloride or other volatile solvents can be used instead of chloroform. The mixture was further dried in vacuum to remove traces of solvent. 8 mL of the solution of either NB A, bromophenol blue, or acid fuchsin in tris buffer (pH 7.2) was added to the test tube with the lipid/monomer mixture and incubated at 35 °C for 30 min. The concentrations of NB A, bromophenol blue, and acid fuchsin in the reaction mixtures were 1.5×10^{-4} M, 5×10^{-3} M, and 3×10^{-3} M, respectively. Bromophenol blue and acid fuchsin are not stable in high-intensity UV light. To minimize the degradation of these dyes during the polymerization process, ascorbic acid was added to the reaction mixture (5 mg/mL). During the hydration of the lipid/monomer mixture, the culture tube was briefly agitated on a Vortexer every 5 min. The suspension was extruded 16 times at 35 °C through a track-etched polyester Nucleopore membrane (Sterlytech) with a 200 nm pore size using a Lipex stainless steel extruder (Northern Lipids).

The sample was irradiated for 1.5 h with UV light ($\lambda = 254$ nm) in a photochemical reactor (10 lamps, 32 W each; the distance between the lamps and the sample was 10 cm) using a quartz tube with a path length of light of approximately 3 mm. The short path length is important for efficient polymerization in the presence of dyes.

Following the polymerization, NaOH in methanol (10 mL, 0.01M) was added to the reaction mixture to precipitate the nanocapsules. The nanocapsules were separated from the reaction mixture and purified in repeated centrifugation and resuspension steps using methanol, a water–methanol mixture, and water as washing solutions.

Preparation of PVA Membranes with Embedded Nanocapsules. An aqueous suspension of nanocapsules (NC) with ~10 mg NC content was centrifuged, and the supernatant was decanted. Precipitated nanocapsules (approximately 10 mg) were dispersed in 1 g of 15% w/w aqueous PVA solution by stirring. Next, 30 μ L of 10% aqueous GDA was added to the suspension. After 30 min of mixing, 45 μ L of 1 M HCl was added to the mixture as an initiator of cross-linking. The mixture was spread on glass slides with 400 μ m thick spacers on the edges and covered with another glass slide. After 30–50 min of polymerization, the solidified PVA membranes on the glass slides were placed into containers filled with deionized water. After 2–3 h the PVA membranes could be easily removed from the glass slides. They were washed with large amounts of water and stored in deionized water containing 0.01% sodium azide to prevent mold growth.

Dynamic Light Scattering (DLS). Hydrodynamic diameter and polydispersity index (PDI) measurements were performed on a Malvern Nano-ZS zetasizer (Malvern Instruments Ltd, Worcestershire, U.K.). The helium–neon laser, 4 mW, was operated at 633 nm, with the scatter angle fixed at 173° and the temperature at 25 °C. Samples (80 μ L) were placed into disposable cuvettes without dilution (70 μ L, 8.5 mm center height Brand UV-Cuvette micro). Each data point was an average of 10 scans.

Spectrophotometry. Most absorbance measurements were performed with an Agilent 8453 photodiode array spectrophotometer using a 1 cm optical path length quartz cuvette equipped with a homemade membrane holder.

For the absorbance measurements of the NB A loaded nanocapsules, an Olis RSM 1000 UV–vis spectrophotometer (Bogart, GA) was used in combination with an integrating

sphere (Olis CLARiTY sample holder). By using a diffuse light beam, the Olis CLARiTY system minimizes or eliminates the interference by light scattering and allows recording spectra in exceedingly turbid samples. The 4 mL volume cuvette was equipped with a stirring bar.

Potentiometry. The diffusion of H^+ or OH^- ions through PVA membranes loaded with nanocapsules was estimated in a homemade transport cell, in which the PVA membrane separated two 9.75 mL volume compartments (Supporting Information, Figure S5). Both compartments were filled with HPLC grade deionized water and were stirred with stirrer bars. Before the transport experiments, the PVA membranes were equilibrated for at least 6 h in deionized water. An instantaneous pH change was introduced on one side of the membrane by spiking the solutions in one of the chambers with 0.25 mL of 1 M HCl or NaOH. After the addition, the concentration of H^+ or OH^- ions in the “source” chamber becomes 0.05 M (pH 1.3 or pH 12.7). The pH change in the other chamber is controlled by the rate of diffusion of H^+ or OH^- ions across the PVA membrane separating the two chambers. This pH change was followed potentiometrically with a Mettler-Toledo InLab 413 combination pH electrode placed into the “receiving” chamber of the transport cell. The combination electrode was connected to an EMF-16 high-input impedance ($>10^{13} \Omega$) data acquisition system (Lawson Laboratories, Inc. Malvern, PA).

Scanning Electron Microscopy. Images were obtained with a Philips XL 30 ESEM scanning electron microscope (Hillsboro, OR). The studied samples were coated with a 12 nm gold–palladium (60:40) layer using EMS 590 X sputter (Hatfield, PA).

RESULTS AND DISCUSSION

The aim of this work was to create a versatile optical sensor platform through the entrapment of vesicle-templated hollow nanocapsules into a permeable matrix. Recently, we reported the directed assembly method for the synthesis of nanocapsules with nanometer-thin walls and molecularly imprinted pores.¹² These capsules can be preloaded with a variety of molecules or nanoparticles before their immobilization into the matrix. The small thickness (~ 1 nm) and high porosity of the walls of the nanocapsules provide ultrafast access to their interior for molecules and ions which are smaller than the diameter of the individual pores.¹¹ However, the porous nanocapsules retain encapsulated reagent molecules with dimensions larger than the diameter of the individual pores.¹³ In this work, we used acrylic nanocapsules formed by the copolymerization of *tert*-butyl methacrylate, butyl methacrylate, and ethylene glycol dimethacrylate in the hydrophobic interior of DMPC-based liposomal bilayers. The UV-initiated free-radical polymerization was done in a similar way to the previously published methods.^{12–14} Photobleaching of the encapsulated dyes was negligible during the formation of the hollow nanocapsules by photopolymerization. The absorbance spectra of dyes showed very little change during 1.5 h of UV irradiation ($\lambda = 254$ nm) (Supporting Information, Figures 1S–3S).

Figure 1 summarizes our approach to an optical sensor platform: pH-sensitive dye molecules are entrapped in porous hollow nanocapsules, and the nanocapsules are embedded in a highly permeable PVA-based hydrogel matrix. In Figure 2, we show examples of the color changes in the nanocapsule-loaded hydrogels upon a step change in the solution pH. To demonstrate the versatility of the immobilization method

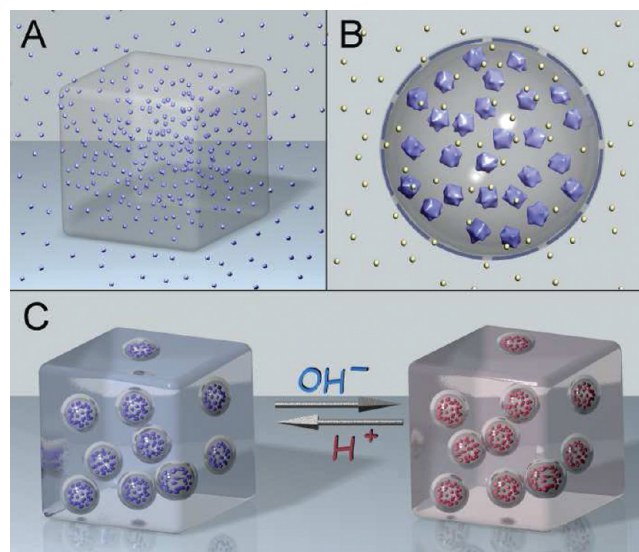


Figure 1. The concept of the sensor platform based on porous, dye-loaded nanocapsules embedded in a highly permeable matrix: (A) low-molecular weight dye molecules leach out from the PVA matrix. (B) Nanocapsules with controlled size nanopores in their walls retain the encapsulated dye molecules but allow free access to their interior for ions or other analytes that are smaller than the diameter of the pores. The size of nanopores can be varied depending on the sizes of the indicator dye and analyte molecules. (C) High-permeability PVA gel cubes with embedded nanocapsules containing entrapped dye molecules. The rate of H^+ and OH^- ion exchange is controlled by the mass transport in the gel.

discussed in this account, we chose Nile blue A (pK_a 9.70), bromophenol blue (pK_a 4.00), and acid fuchsin (transition pH 12.0–14.0) as representative pH-sensitive dyes for the entrapment into the nanocapsules.

As shown in the scanning electron microscopy (SEM) images of Figure 3, the nanocapsules are distributed fairly homogeneously throughout the hydrogel matrix. The images also show that the nanocapsules retain their spherical shape in the PVA gel and do not aggregate or phase separate from the hydrogel.

In our earlier work, we showed that dye-loaded nanocapsules change color rapidly upon changing the pH in their environment.¹¹ Using the stopped-flow technique, we showed that the rates of protonation and deprotonation were the same for free dyes and dyes encapsulated inside polymer nanocapsules prepared by controlled polymerization of *t*-butylstyrene and divinylbenzene in the interior of liposomal bilayers.¹¹ On the basis of these observations, we concluded that the transport of ions across the capsule boundary was not the rate-limiting step in the optical response. To confirm that the rate of protonation is similarly fast when the pH indicator dyes are encapsulated in the nanocapsules prepared by copolymerization of butyl methacrylate, *tert*-butyl methacrylate, and ethylene glycol dimethacrylate, as it is described in this work, we recorded the change in the absorbance spectra of solutions with NB A, bromophenol blue, and acid fuchsin loaded nanocapsules (~ 1 mg/mL of nanocapsules containing the dye with concentration of 1.5×10^{-4} M) following a step change in the solution pH. Figure 4 shows the time dependent changes in the absorbance when 0.1 mL of 1 M HCl (or 0.1 mL of 1 M NaOH or 0.1 mL of 2 M HCl) was injected into the stirred spherical cuvette of the Olis CLARiTY spectrophotometer filled with 3.9

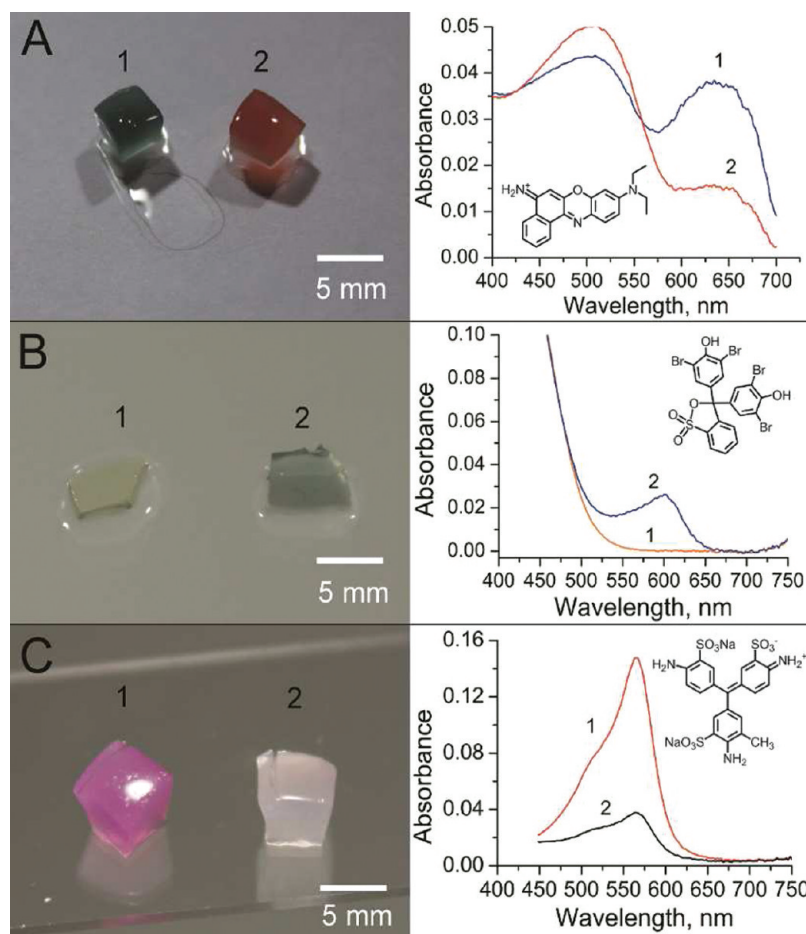


Figure 2. Color and spectral changes in the nanocapsule-loaded films upon a step change in the solution pH. The nanocapsules were loaded with (A) Nile blue A, (B) bromophenol blue, and (C) acid fuchsin. The labels 1 and 2 indicate solutions with pH 3 and pH 10 (for parts A and B) and pH 7 and pH 13.5 (for part C), respectively. Left column: Photographs of PVA hydrogel cubes containing the different dye-loaded nanocapsules in solutions 1 and 2. Right column: Corresponding absorption spectra along with the structures of the encapsulated dyes. The traces labeled with 1 and 2 were recorded in solutions 1 and 2.

mL 0.01 M NaOH (or 0.01 M HCl or 0.05 M NaOH) containing the nanocapsules loaded with different dyes. Figure 4S in the Supporting Information shows a three-dimensional time-resolved absorbance measurement. The rate of the color change was essentially the same when HCl (0.1 M) was added to a solution of free NB A in 0.01 M NaOH (data not shown), i.e., in this experiment the mixing rate controlled the rate of the absorbance change. In agreement with this statement, the rate of the absorbance change was the same with bromophenol blue and acid fuchsin loaded capsules.

To determine the rate of the color change of dye-loaded nanocapsules in PVA-based hydrogels, ~0.4 mm thick, fully hydrated PVA films were clamped by a home-built specimen holder, which was inserted into a standard 1 cm cuvette. The specimen holder positioned the PVA film in the middle of the cuvette orthogonal to the light path. At time zero, the cuvette was filled with either 0.05 M HCl or 0.05 M NaOH, and the rate of protonation or deprotonation of the encapsulated dye in the PVA film was followed by recording the absorbance at 665 nm as a function of time. As shown in Figure 5, the 90% response time of a ~0.4 mm thick nanocapsule-loaded PVA film is around 60 s following a sudden pH increase or decrease in the sample solution. The rate of color change is significantly slower when the dye-loaded nanocapsules are entrapped in the PVA membranes (Figure 5) compared when they are

suspended in an aqueous solution (Figure 4). This decrease in the rate of color change is due to the relatively sluggish, diffusion-controlled equilibration process within the PVA film. To confirm this statement, we determined the transport rate of H_3O^+ ions across PVA membranes loaded with empty nanocapsules.

In these experiments, the PVA membrane containing empty nanocapsules was clamped between two solution compartments filled with deionized water. At time zero, an instantaneous pH change was introduced on one side of the membrane while the pH change on the other side of the membrane was monitored with a glass electrode. As expected, the time constant of the recorded transients is a quadratic function of the membrane thickness. The 90% response time with a ~0.2 mm thick PVA membrane is approximately 4 times shorter than with a ~0.4 mm thick membrane. The transients recorded in the membrane separated transport cell with ~0.2 and ~0.4 mm thick membranes are shown in Figure S5 in the Supporting Information. The comparison of Figure 5 and Figure S5 in the Supporting Information shows an apparently faster response in the spectrophotometric than in the potentiometric experiment, although the membrane thicknesses were the same. In fact, the difference in the recorded rates is a reflection of the difference in the experimental conditions. In the spectrophotometric experiment (Figure 5), the pH change is introduced on

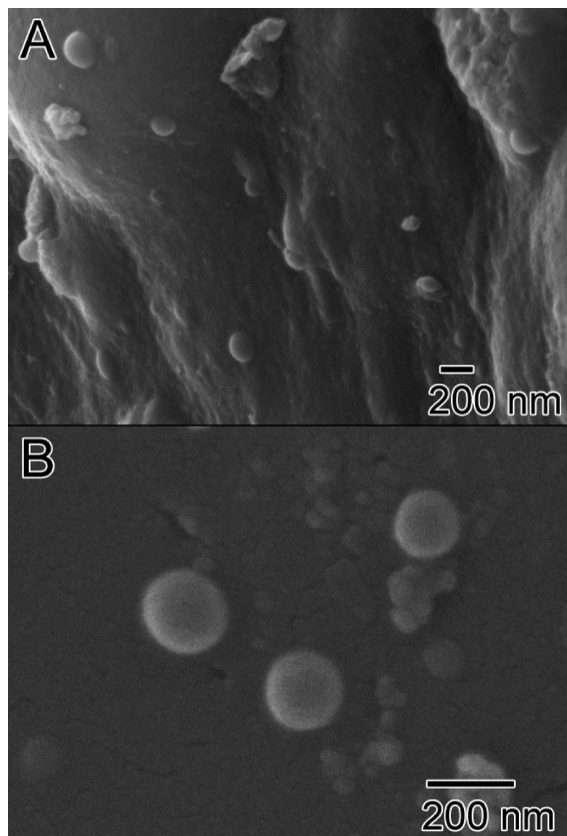


Figure 3. SEM images of PVA hydrogels with embedded nanocapsules. (A) The image shows a surface of a freeze-dried hydrogel specimen, which has been broken off a gel sample. (B) The image shows a microtome-cut surface of a freeze-dried hydrogel.

both sides of the membrane simultaneously, and the gradual protonation/deprotonation process in the membrane is recorded, while in the potentiometric experiment (Figure S5) a step change in the solution pH on one side of the membrane is followed by monitoring pH in the bathing solution on the other side of the membrane.^{15–17}

Kinetic data, discussed above, indicate that decreasing the thickness of the hydrogel film can drastically shorten the response time of optical sensors based on hydrogels loaded with pH-sensitive nanocapsules. By reducing the PVA membrane thickness to a few micrometers, response times in the range of a tens to hundreds of milliseconds are expected. Using these thin sensing films on the surface of optical waveguides is expected not only to result in short response times but also provide large sensitivity. With \sim 100 nm penetration depth of an evanescent wave, a few centimeters long waveguide would generate a signal corresponding to the effective optical path length of several millimeters.

In our previous work, we showed that Procion Red (MW 615) was retained within porous nanocapsules without a measurable loss for over 240 days.¹³ Since the nanocapsules cannot leach out from the PVA matrix, optical sensing films containing immobilized dye-loaded porous nanocapsules are expected to have good stability and an extended lifetime. In Figure 6, we show the reproducibility of the optical response of a \sim 0.4 mm thick PVA membrane containing NB A loaded nanocapsules upon its exposure to a pH 2.5 citrate buffer (0.02 M). After the exposure to the citrate buffer and before recording the next transient, the membrane was washed with a

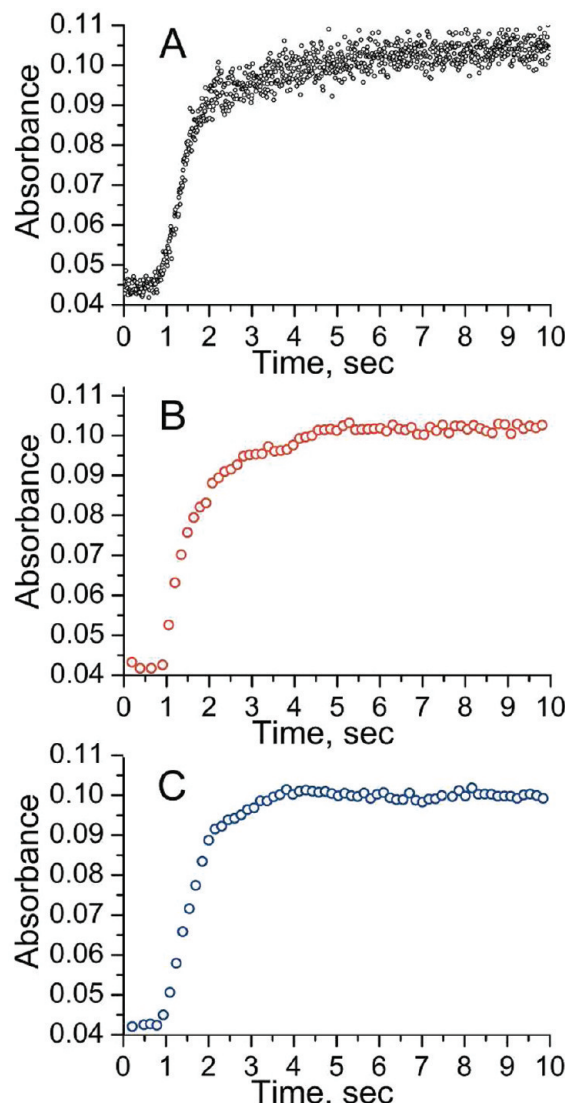


Figure 4. Transient changes in the absorbance of solutions with dispersed dye-loaded nanocapsules (1 mg/mL) upon injecting 0.1 mL of 1 M HCl (A) or 0.1 mL of 1 M NaOH (B) or 0.1 mL of 2 M HCl (C) into the stirred cuvette ($V = 4$ mL) of the OLIS CLARiTY spectrophotometer filled with 3.9 mL of suspension of nanocapsules in 0.01 M aqueous NaOH (A), or 0.01 M aqueous HCl (B), or 0.05 M aqueous NaOH (C). The nanocapsules were loaded with (A) NB A, (B) bromophenol blue, and (C) acid fuchsin. The traces were recorded at 665 nm for part A, 605 nm for part B, and 570 nm for part C. The sampling rates and integration times were 1000 Hz and 1 ms for part A and 100 Hz and 10 ms for parts B and C, respectively.

large amount of deionized water (>25 mL), equilibrated with pH 7.5 tris buffer (0.05 M), and rinsed with deionized water again. The vertical dashed lines in Figure 6 indicate the washing cycles between the transient measurements. The reproducibility of the transients proves that the performance of the sensors is not compromised upon extended exposure to large volumes of aqueous solutions and to lengthy illumination, i.e., the dye-loaded nanocapsules are retained in the PVA film and the dye did not show degradation related to photobleaching.

The stability of the PVA-based optical sensor membranes, hydrogels containing dye-loaded nanocapsules, was confirmed by “leaching” studies. In these experiments, the PVA-based hydrogel membranes were exposed to water and methanol for

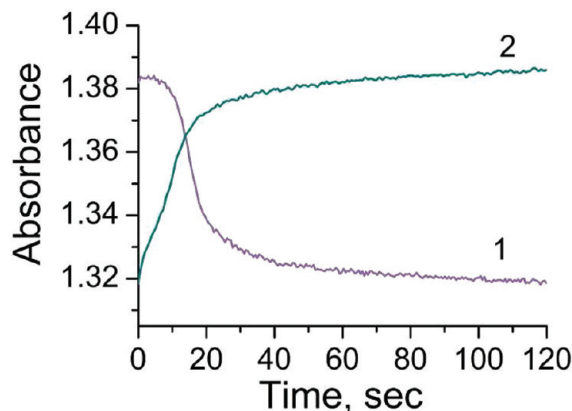


Figure 5. Time dependent changes in the absorbance of a ~ 0.4 mm thick PVA film loaded with NB A filled porous nanocapsules following a pH change in the bathing solution. (1) A PVA film equilibrated in 0.05 M HCl exposed to 0.05 M NaOH and (2) a PVA film equilibrated in 0.05 M NaOH exposed to 0.05 M HCl.

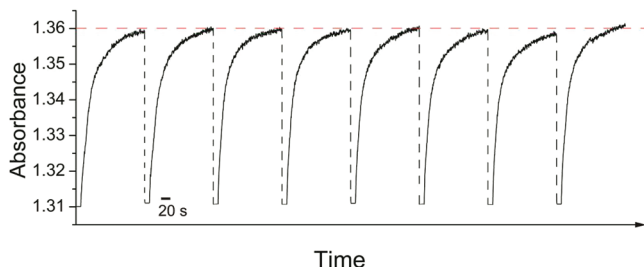


Figure 6. Traces of the transient absorbance changes recorded at 665 nm upon the repeated exposure of a pH-sensitive PVA membrane containing NB A loaded nanocapsules to pH 2.5 citrate (0.02 M) buffer. The membrane was clamped in a membrane holder which is inserted into the cuvette. The transient changes in the PVA membrane absorbance were recorded upon filling the cuvette with the pH 2.5 citrate buffer. Between the individual measurements, the membrane was thoroughly washed with DI water and equilibrated with pH 7.5 tris buffer.

at least 2 weeks. During this time period, the absorbance spectra of the supernatant was repeatedly recorded. These absorbance spectra did not indicate any dye leaching in the presence of PVA-based membranes with the encapsulated dye (Supporting Information, Figure 6S). However, the free (unencapsulated) dye molecules leached out rapidly from the PVA hydrogels prepared under identical conditions.

Encapsulation of NB A into polymer nanocapsules significantly increased its stability. Phenoxazine derivatives, like NB A, are known to be sensitive to photochemically initiated oxidation which is widely utilized in photodynamic therapy.^{18–21} When the dye is excited by red light, the photo oxidation can proceed with different mechanisms,²² resulting in rapid degradation of the dye molecules. In Figure 7 we show pictures of freshly prepared NB A solutions (2×10^{-5} M) with pH values ranging between pH 2.5 and pH 12.5 and pictures of the same solutions after they were exposed to ambient laboratory light for 2 weeks. The comparison of the two snapshots indicates almost complete degradation of the dye in all of the solutions. The degradation is also apparent through the emergence of a precipitate on the bottom of some of the test tubes (e.g., Figure 7, sample 6). The pH in test tubes 1–9 was set with citrate- (pH 2.5, 3.5), MES- (2-(*N*-morpholinoethanesulfonic acid) (3.4), borate- (5,6,7), and phosphate-based (8, 9) buffers, respectively.

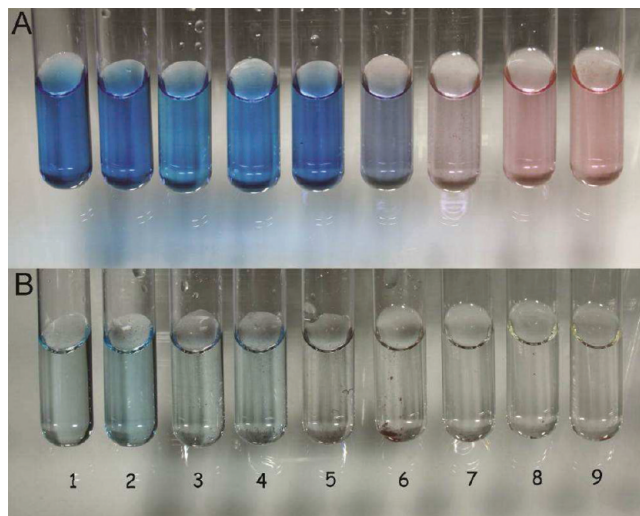


Figure 7. Photostability of 2×10^{-5} M NB A in buffers solutions with pH values ranging between pH 2.5 and 12.5: (A) photos of freshly prepared solutions; (B) photos of the same solutions after 2 weeks of storage under regular laboratory conditions. The pH in test tubes 1–9 was set to pH 2.5, 3.5, 5.5, 6.5, 9.5, 10.0, 10.5 11.5, and 12.5 using citrate- (1,2), MES- (2-(*N*-morpholinoethanesulfonic acid) (3,4), borate- (5,6,7), and phosphate-based (8, 9) buffers, respectively.

(ethanesulfonic acid) (pH 5.5, 6.5), borate- (pH 9.5, 10.0, 10.5), and phosphate-based (pH 11.5, 12.5) buffers. Previously, we showed that the photochemical stability of certain Nile blue A derivatives, commonly used in ion selective membranes, depends both on the pH and the composition of the solution.²³ The rate of photochemical decomposition is facilitated by the presence of certain anions (e.g. tetraphenylborate, Br^- , I^- , Cl^-) while the protonated form of the dye is quite stable in the presence of NO_3^- , ClO_4^- , etc.

In contrast to the free dye, the encapsulated NB A had remarkable stability. As shown in Figure 8, the NB A loaded nanocapsules suspended in buffer solutions or embedded in

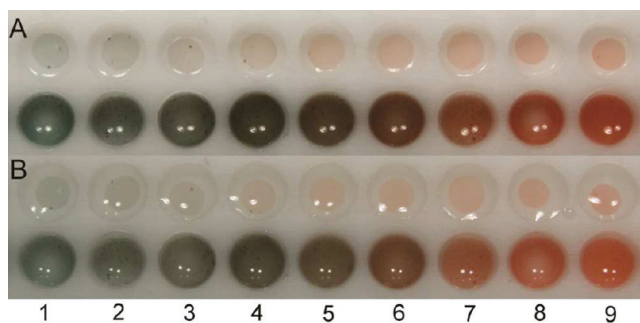


Figure 8. Photostability of NB A when encapsulated in porous nanocapsules. The upper rows in parts A and B are photographs of microplate wells filled with PVA-based hydrogel specimens in which the NB A loaded nanocapsules are dispersed. The hydrogel specimens are in contact with buffer solutions of different pH values. The lower rows in parts A and B are photographs of microplate wells filled with buffer solutions of different pH values in which the NB A loaded nanocapsules are dispersed. (A) Freshly prepared samples, (B) the same samples after 2 weeks at regular laboratory conditions. The pH in the wells labeled 1–9 was set to pH 2.5, 3.5, 5.5, 6.5, 9.5, 10.0, 10.5 11.5, and 12.5 using citrate- (1,2), MES- (2-(*N*-morpholinoethanesulfonic acid) (3,4), borate- (5,6,7), and phosphate-based (8, 9) buffers, respectively.

PVA-based hydrogel had no change in their color intensity over the same 2-week period and the same ambient conditions. Compartmentalization of NB A significantly enhanced its stability both in buffers and hydrogels.

Entrapment of encapsulated NB A in a PVA hydrogel affected the pH value of the color change of the dye. The pH value of the color change of indicator dyes is related to their pK_a values. The pH value of 50% protonation is equal to the pK_a , corresponding to the half-transition point of the indicator dye. The pK_a of NB A in aqueous buffer solutions is 9.7.²⁴ The color change of encapsulated NB A dispensed in a solution or embedded in a PVA matrix occurs at lower pH compared to the free dye (Figure 8A). A similar matrix effect, although in the opposite direction of the pH change, was observed when bromophenol blue (BPB) was entrapped in a sol–gel matrix.²⁵ The pK_a of BPB shifted from 3.93 to 6.4 when the dye was embedded into a sol–gel matrix. The influence of immobilization on the absorption properties of different dyes²⁶ opens opportunities to tune the response range of the nanocapsules-based optical sensors through the selection of polymeric matrix and/or by coentrainment of counterions with the dye molecules into the porous nanocapsules at different concentrations.

CONCLUSIONS

During the optimization of the sensing membranes of conventional optodes, researchers often have to compromise between the short response time and long lifetime. In this work, a versatile sensor platform is presented with dual immobilization protocol. The indicator dyes are entrapped in hollow nanocapsules with nanometer-thin walls of controlled porosity, and the dye-loaded nanocapsules are immobilized in a high-permeability PVA matrix. This approach provides robust sensing films with fast response, minimal drift, good reproducibility, and extended lifetime. The controlled porosity nanocapsules with the nanometer-thin walls (i) increase the photostability of the encapsulated dyes, (ii) prevent their leaching from the sensing membrane, but (iii) allow ultrafast transport of the analyte through the capsule boundary. The successful encapsulation of a broad range of pH-sensitive dyes points to a variety of potential applications.

The nanocapsules are immobilized in a PVA-based hydrogel matrix, which makes their deposition onto the tip of optical fibers or the surface of waveguides feasible. The rate of response of the optical sensors with dye-loaded porous nanocapsules in a high porosity PVA matrix is controlled by the membrane thickness. With ~400 μm thick sensing films, the response times are in the range of 40–60 s. Since the rate of response is a quadratic function of the membrane thickness, reducing the membrane thickness to a few micrometers should lead to response times in the millisecond range.

ASSOCIATED CONTENT

Supporting Information

Additional information as noted in text. This material is available free of charge via the Internet at <http://pubs.acs.org>.

AUTHOR INFORMATION

Corresponding Author

*E-mail: elindner@memphis.edu (E.L.); epinkhas@slu.edu (E.P.).

Notes

The authors declare no competing financial interest.

ACKNOWLEDGMENTS

This work was supported by FedEx Institute of Technology and National Science Foundation (Grant CHE-1012951), and Saint Louis University Presidential Research Fund Award. We thank Dr. Richard DeSa (Olis, Inc.) for help with absorbance measurements.

REFERENCES

- (1) Bakker, E.; Bühlmann, P.; Pretsch, E. *Chem. Rev.* **1997**, *97*, 3083–3132.
- (2) Bühlmann, P.; Pretsch, E.; Bakker, E. *Chem. Rev.* **1998**, *98*, 1593–1687.
- (3) Janata, J. *Anal. Chem.* **1987**, *59*, 1351–1356.
- (4) Seiler, K. *Ion-Selective Optode Membranes*; Fluka Chemie AG: Buchs, Switzerland, 1993.
- (5) Walters, J. D.; Hall, E. A. H. *Analyst* **2011**, *136*, 4718–4723.
- (6) Ruedas-Rama, M. J.; Hall, E. A. H. *Analyst* **2006**, *131*, 1282–1291.
- (7) Lee, Y.-E. K.; Smith, R.; Kopelman, R. *Annu. Rev. Anal. Chem.* **2009**, *2*, 57–276.
- (8) McDonagh, C.; Burke, C. S.; MacCraith, B. D. *Chem. Rev.* **2008**, *108*, 400–422.
- (9) Jerónimo, P. C. A.; Araújo, A. N.; Conceição B. S. M. Montenegro, M. *Talanta* **2007**, *72*, 13–27.
- (10) Wright, J. D.; Sommerdijk, N. A. *Sol-Gel Materials: Chemistry and Application*; CRC Press: Boca Raton, FL, 2000.
- (11) Dergunov, S. A.; Miksa, B.; Ganus, B.; Lindner, E.; Pinkhassik, E. *Chem. Commun.* **2010**, *46*, 1485–1487.
- (12) Danila, D. C.; Banner, L. T.; Karimova, E. J.; Tsurkan, L.; Wang, X. Y.; Pinkhassik, E. *Angew. Chem., Int. Ed.* **2008**, *47*, 7036–7039.
- (13) Dergunov, S. A.; Kesterson, K.; Li, W.; Wang, Z.; Pinkhassik, E. *Macromolecules* **2010**, *43*, 7785–7792.
- (14) Dergunov, S. A.; Pinkhassik, E. *Angew. Chem., Int. Ed.* **2008**, *47*, 8264–8267.
- (15) Lindner, E.; Zwicke, T.; Bakker, E.; Lan, B. T. T.; Tóth, K.; Pretsch, E. *Anal. Chem.* **1998**, *70*, 1176–1181.
- (16) Schneider, B.; Zwicke, T.; Federer, B.; Pretsch, E.; Lindner, E. *Anal. Chem.* **1996**, *68*, 4342–4350.
- (17) Zwicke, T.; Schneider, B.; Lindner, E.; Sokalski, T.; Schaller, U.; Pretsch, E. *Anal. Sci.* **1998**, *14*, 57–61.
- (18) Dass, C.; Thimmaiah, K. N.; Jayashree, B. S.; Seshadri, R.; Israel, M.; Houghton, P. J. *Biol. Mass Spectrom.* **1994**, *23*, 140–146.
- (19) Diwu, Z.; Lown, J. W. *Pharmacol. Ther.* **1994**, *63*, 1–35.
- (20) Geze, M.; Morliere, P.; Maziere, J. C.; Smith, K. M.; Santus, R. J. *Photochem. Photobiol. B* **1993**, *20*, 23–35.
- (21) Lin, C. W.; Shulok, J. R.; Wong, Y. K.; Schanbacher, C. F.; Cincotta, L.; Foley, J. W. *Cancer Res.* **1991**, *51*, 1109–1116.
- (22) Wilkinson, F.; Helman, W. P.; Ross, A. B. *J. Phys. Chem. Ref. Data* **1993**, *22*, 113–262.
- (23) Langmaier, J.; Lindner, E. *Anal. Chim. Acta* **2005**, *543*, 156–166.
- (24) Sabnis, R. W. *Handbook of Acid-Base Indicators*, CRC Press: Boca Raton, FL, 2007.
- (25) Lindner, E.; Bordelon, D.; Kim, M. D.; Dergunov, S. A.; Pinkhassik, E.; Chaum, E. *Electroanalysis* **2012**, *24*, 42–52.
- (26) Reisfeld, R.; Jorgensen, C. K. *Struct. Bonding (Berlin, Ger.)* **1992**, *77*, 207–265.